The hydrophobic lock-and-key intersubunit motif of glutathione transferase A1-1: implications for catalysis, ligandin function and stability

Yasien Sayed, Louise A. Wallace, Heini W. Dirr*

Protein Structure-Function Research Programme, Department of Molecular and Cell Biology, University of the Witwatersrand, Johannesburg 2050, South Africa

Received 26 October 1999; received in revised form 14 December 1999

Edited by Hans Eklund

Abstract A hydrophobic lock-and-key intersubunit motif involving a phenylalanine is a major structural feature conserved at the dimer interface of classes alpha, mu and pi glutathione transferases. In order to determine the contribution of this subunit interaction towards the function and stability of human class alpha GSTA1-1, the interaction was truncated by replacing the phenylalanine 'key' Phe-51 with serine. The F51S mutant protein is dimeric with a native-like core structure indicating that Phe-51 is not essential for dimerization. The mutation impacts on catalytic and ligandin function suggesting that tertiary structural changes have occurred at/near the active and non-substrate ligand-binding sites. The active site appears to be disrupted mainly at the glutathione-binding region that is adjacent to the lock-and-key intersubunit motif. The F51S mutant displays enhanced exposure of hydrophobic surface and ligandin function. The lock-and-key motif stabilizes the quaternary structure of hGSTA1-1 at the dimer interface and the protein concentration dependence of stability indicates that the dissociation and unfolding processes of the mutant protein remain closely coupled.

Key words: Glutathione transferase; Subunit interaction; Ligandin function; Conformational stability; Protein folding

1. Introduction

The glutathione transferases (EC 2.5.1.18) are a supergene family of dimeric enzymes that metabolize a broad range of structurally diverse non-polar electrophiles [1]. Cytosolic GSTs exist as stable dimeric structures of M_r ~50 000 and can be divided into seven species-independent gene classes [2–6]. They share a similar overall folding topology [2] with each polypeptide chain arranged into two structurally distinct domains. A dimeric quaternary structure is required for the formation of a fully functional active site part of which is located near the subunit interface. Examination of the structural features at the subunit interfaces of the various gene classes reveals the existence of two major types of interfaces; namely, the alpha/mu/pi/Sj26GST type and the sigma/theta type. The subunit interfaces of the former group have a curved topography and are hydrophobic with few polar interactions. Furthermore, there is a conserved hydrophobic interaction formed by the side chain of a phenylalanine residue (F51 in alpha; F56 in mu; F46 in pi) that protrudes from a loop in domain I of one monomer into a hydrophobic pocket between α-helices 4 and 5 of domain II of the other monomer (Fig. 1). This lock-and-key type motif physically anchors the two subunits together at either ends of the interface. In contrast, the class sigma/theta subunit interface is flat and hydrophilic with an extensive network of polar interactions and lacks the hydrophobic lock-and-key motif. The nature of the dimer interface can impact on the conformational stability and folding of GSTs [7,8].

In the present study, a F51S mutant of human glutathione transferase class alpha with two type-1 subunits (hGSTA1-1) was engineered to assess the contribution of the hydrophobic lock-and-key subunit interaction toward the catalytic and ligandin function as well as protein conformational stability. The results demonstrate that F51 is an important structural moiety in modulating catalytic and ligandin functions and although not essential for dimerization, it maintains conformational stability of the dimeric structure of the protein.

2. Materials and methods

2.1. Materials

Heterologously-expressed wild-type human GSTA1-1 (hGSTA1-1) was purified from the plasmid pKHA1/JM103. The plasmid was a kind gift from Prof. B. Mannervik [9]. PCR-based double-stranded DNA site-directed mutagenesis was performed using the ExSite mutagenesis kit from Stratagene. The diagnostic restriction enzyme *Eco*RV (Amersham Life Sciences International) was used to screen for mutant plasmid DNA. The oligonucleotide primers used to generate the F51S point mutation in hGSTA1-1 were: (1) F51S FWD primer: 5′-GGATATCTGATG***TCC***CAGCAAGTGCCAATG-3′ and (2) F51S REV primer: 5′-ATCATTTCTTAACTTGTCCAAATG-3′ where the underlined nucleotides in the F51S FWD Primer indicates the diagnostic *Eco*RV site (a translationally silent mutation utilized for screening mutant plasmid DNA) and the bold print in italics represents the mutation that will generate the phenylalanine to serine mutation at position 51 in the pKHA1 plasmid DNA. The entire cDNA region of pKHA1 encoding the F51S mutation was sequenced using an ABI Prism 310 Genetic analyzer from PE Biosystems to ensure the absence of any undesirable mutations that may have occurred during PCR. Ultrapure urea was purchased from ICN Biomedicals. All other reagents were of analytical grade.

2.2. Expression and purification of hGSTA1-1

The wild-type hGSTA1-1 protein was purified using *S*-hexylgluta-

*Corresponding author. Fax: (27)-11-403 1733.
E-mail: 089dirr@cosmos.wits.ac.za

Abbreviations: hGSTA1-1, human glutathione transferase class alpha with two type-1 subunits; ANS, anilinonaphthalene sulfonate; CDNB, 1-chloro-2,4-dinitrobenzene; SDS-PAGE, sodium dodecyl sulfate-polyacrylamide gel electrophoresis; SEC-HPLC, size exclusion-high performance liquid chromatography

PII: S0014-5793(99)01747-0

thione affinity chromatography as described previously [9,10]. The mutant plasmid DNA was transformed into *E. coli* BL21 cells containing the pLysS plasmid. The F51S mutant protein displayed a reduced affinity towards the *S*-hexylglutathione affinity matrix and was purified on a CM-Sephadex cation exchange column pre-equilibrated with 10 mM sodium phosphate buffer, pH 7.4, 1 mM EDTA and 0.02% sodium azide. The adsorbed protein was eluted from the CM-column using a 0–0.3 M sodium chloride gradient. The protein was subsequently concentrated and buffer-exchanged into protein storage buffer (20 mM sodium phosphate buffer, pH 6.5, 0.1 M sodium chloride, 1 mM EDTA and 0.02% sodium azide). The purity of both the wild-type and F51S mutant proteins was assessed to be >95% by sodium dodecyl sulfate-polyacrylamide gel electrophoresis (SDS-PAGE) and size exclusion-high performance liquid chromatography (SEC-HPLC). Protein concentration of the wild-type and F51S proteins was estimated spectrophotometrically at 280 nm using a molar extinction coefficient of 38 200 M^{-1} cm^{-1} [11].

2.3. Spectroscopic measurements

The intrinsic fluorescence of the lone tryptophan (Trp-20) in hGSTA1-1 was measured in a Hitachi model 850 fluorescence spectrofluorimeter as described previously [11] using an excitation at 295 nm. The exposure of Trp-20 to solvent in the wild-type and F51S mutant hGSTA1-1 was monitored using acrylamide quenching as detailed in [12]. Far-UV circular dichroism measurements were made in the Applied Photophysics circular dichroism accessory (CD.2C) with a 2 mm pathlength. The instrument was calibrated using (1*S*)-(+)-10-camphorsulfonic acid.

2.4. Functional studies

Enzyme activity and kinetic parameters for wild-type and F51S mutant proteins were determined with reduced glutathione (1–150 mM) and 1-chloro-2,4-dinitrobenzene (CDNB) (0.1–2mM) at pH 6.5 (final ethanol per reaction was 3.3%) as described previously [13].

Non-substrate ligand binding (i.e. ligandin function) of hGSTA1-1 in the absence and presence of glutathione (adjusted to pH 6.5) was assessed by the interaction between protein (1 μM) and the anionic ligand anilinonaphthalene sulfonate (ANS) by fluorescence techniques (excitation at 390 nm) as described previously [14].

2.5. Equilibrium unfolding studies

Reversibility and equilibrium unfolding studies were carried out as detailed in [11]. Protein and urea concentration ranges were 0.22–2.2 μM and 0–8 M, respectively. Structural changes were monitored by tryptophan fluorescence (emission at 325 nm for folded protein and 355 nm for unfolded protein) and by far-UV circular dichroism at 222 nm. Due to the low specific activity of the F51S mutant it was not possible to use enzyme activity as a functional probe during unfolding. Analysis of the urea-induced equilibrium unfolding transition was performed according to [11,15] for the determination of the unfolding parameters $\Delta G(H_2O)$ and *m*-value.

3. Results

3.1. Structural characterization of F51S mutant hGSTA1-1

SDS-PAGE and SEC-HPLC data confirmed that the F51S mutant protein was homodimeric with a molecular mass of 54 kDa. Furthermore, far-UV circular dichroism spectra indicated no significant change in the secondary structure of F51S mutant hGSTA1-1 (data not shown; for example of CD spectrum for hGSTA1-1, see [25]). Fluorescence spectral properties indicated an identical emission maximum at 325 nm for both wild-type and mutant proteins, while the F51S mutant protein exhibited a slightly reduced fluorescence intensity. Steady-state anisotropy studies indicate similar mobilities for Trp-20 in the mutant protein (anisotropy of 0.10) and wild-type protein (anisotropy of 0.11). The ability of acrylamide to quench Trp-20 fluorescence is a useful way of determining the exposure of Trp-20 to the solvent. Stern–Volmer plots at low acrylamide concentrations (0–0.3 M) were linear and yielded K_{sv} values of 2.1 M^{-1} ($r^2 = 0.998$) and 3.1 M^{-1} ($r^2 = 0.997$) for wild-type and mutant proteins, respectively.

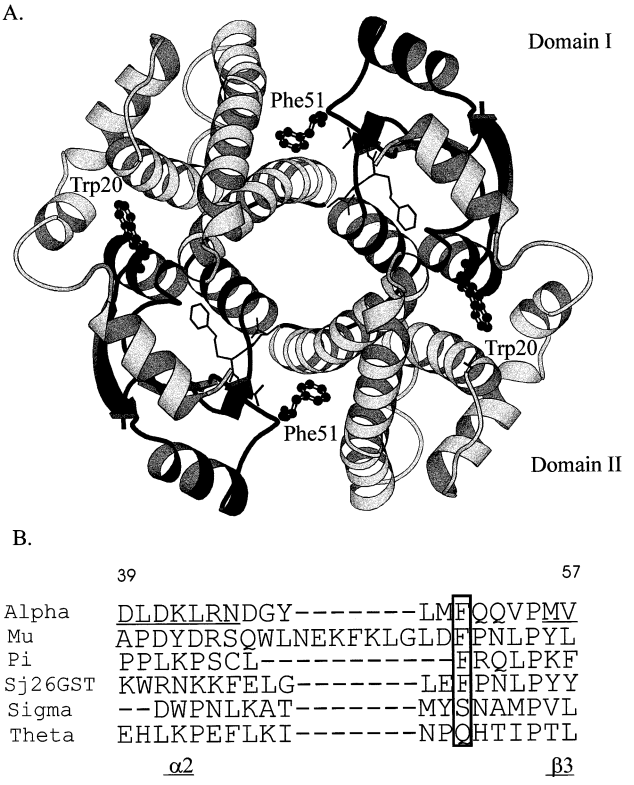

Fig. 1. A: Ribbon representation of human class alpha GSTA1-1 viewed down the two-fold axis [20]. The location of Phe-51 and Trp-20 are represented as a ball-and-sticks. The active site ligands are shown in bold. B: Indicates the sequence alignment of topologically equivalent residues from representatives of the various gene classes for which crystal structures are known. The residue numbering shown above the sequences is for hGSTA1-1. The boxed-in residues refer to the conserved phenylalanine residue in class alpha/mu/pi/Sj26 GSTs and topologically equivalent residues in classes sigma and theta. The underlined residues in hGSTA1-1 are located in secondary structural elements, where α refers to α-helix and β refers to β-strand.

3.2. Catalytic properties

The specific activity of the F51S mutant protein was only 3% of that displayed by wild-type hGSTA1-1. The estimated values of K_m and V_{max} for reduced glutathione were 1.3 mM and 0.13 μmol min^{-1} ($r^2 = 0.95$) for wild-type protein, and 70 mM and 0.14 μmol min^{-1} ($r^2 = 0.91$) for F51S mutant protein. The K_m and V_{max} values for the electrophilic substrate CDNB were estimated to be 0.4 mM and 0.15 μmol min^{-1} ($r^2 = 0.8$) for wild-type protein and 1.6 mM and 0.10 μmol min^{-1} ($r^2 = 0.95$) for F51S mutant protein.

3.3. ANS ligandin function

The anionic dye ANS binds a site at the dimer interface of hGSTA1-1 [16,17]. The dye can be utilized as a probe to monitor the appearance/disappearance of hydrophobic patches or surfaces on proteins that are undergoing structural changes [18]. In the absence of protein, ANS exhibits an emission maximum at 535 nm. The emission spectrum for protein-bound ANS is blue-shifted to 480 nm (wild-type) and 473 nm (mutant). This shift is accompanied by enhanced ANS fluorescence intensity (which is 6.5-fold greater for mutant when

compared to that for wild-type protein). The F51S mutant protein binds ANS approximately three times stronger than the wild-type protein; $K_d = 18.7$ μM ($r^2 = 0.998$) compared with $K_d = 55.1$ μM ($r^2 = 0.98$) for the wild-type. Fig. 2 shows the effect of glutathione on ANS binding. In the absence of glutathione, F51S displays enhanced binding of ANS (relative to that seen for wild-type). This binding is diminished substantially by the presence of glutathione (reduced approximately three-fold at 100 mM glutathione). There was no change in the emission maximum wavelength (at 473 nm) of ANS bound to the mutant. On the other hand, binding of glutathione to the G-site of the wild-type protein enhanced the binding of ANS. This was accompanied by a shift in the emission maximum wavelength from 480 to 475 nm.

3.4. Conformational stability

Urea-induced unfolding was reversible with recoveries of >90% for fluorescence of refolded wild-type and F51S mutant proteins. The F51S mutant unfolds through a single sigmoidal transition which, when compared to that for the wild-type protein, occurs at lower urea concentrations but over a slightly broader concentration range (Fig. 3). Data from Trp-20 fluorescence and ellipticity at 222 nm measurements are essentially superimposable suggesting coincident changes in secondary and tertiary structures. The midpoint of the transition for F51S mutant protein is 4.1 M urea compared with 4.5 M urea for wild-type enzyme (both at 1 μM). Fitting the data for the mutant protein according to [11,15] yielded a $\Delta G(H_2O)$ of 16.8 kcal mol^{-1} and an *m*-value of 2.1 kcal mol^{-1} M^{-1} urea which are significantly different from the values for the wild-type (27.5 kcal mol^{-1} and 4.2 kcal mol^{-1} M^{-1} urea, respectively [11]). The protein concentration dependence of the unfolding data (inset of Fig. 3) indicates increasing protein stability with increasing protein concentration.

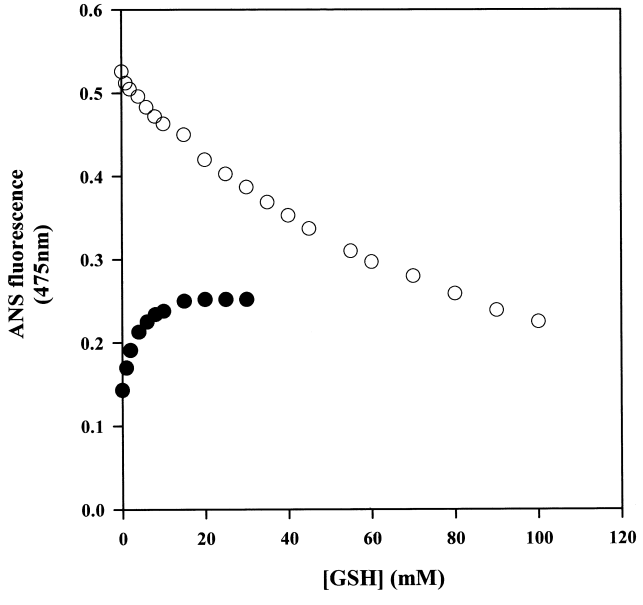

Fig. 2. The effect of glutathione on the binding of ANS to the wild-type (●) and the F51S mutant (○) protein.

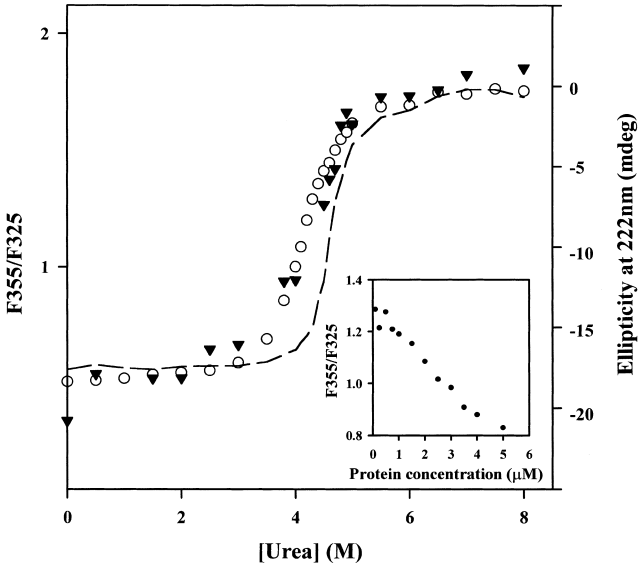

Fig. 3. F51S mutant protein conformational stability studies. Urea-induced equilibrium unfolding monitored by Trp-20 fluorescence (○) and ellipticity at 222 nm (▼) for 2 μM F51S mutant protein. The unfolding curve for wild-type protein is shown by the broken line. Inset: protein concentration dependence of the stability of F51S mutant protein. Protein at different concentrations was incubated in 4.1 M urea (i.e. the Cm-value for 2 μM mutant protein) and the fluorescence intensity measured at 355 nm (unfolded) and 325 nm (folded).

4. Discussion

The dimerization of GST subunits involves contacts formed primarily between domain I of one subunit and domain II of the other subunit [2]. Studies with mammalian [7,11,12] and schistosomal [19] GSTs indicate that the intersubunit interactions are a significant source of stabilization not only for the association of subunits but also for the tertiary structures of the individual subunits. Class alpha/mu/pi/sj26 GSTs have a conserved lock-and-key interaction motif at either end of their subunit interfaces (see Fig. 1A for class alpha). The side chain of a phenylalanine in a loop of domain I functions as a key which extends across the dimer interface and locks into a hydrophobic pocket formed between α-helices 4 and 5 in domain II of the opposite subunit. Presently, nothing is known about the role of this intersubunit lock-and-key motif in dimerization/dimer stability and in maintaining competent conformations for GST catalytic and ligandin functions.

In the present study, the F51S mutant of hGSTA1-1 was found to be dimeric indicating that the lock-and-key intersubunit motif is not essential for dimerization to occur. In this regard, it is interesting to note that the more primitive class sigma and theta GSTs, which lack this structural motif, also form functional dimers (see [21]). The F51S mutation in hGSTA1-1 does not appear to have any significant impact on the secondary structure of the protein as well as the intrasubunit domain I-domain II interface (for which Trp-20 is a sensitive probe [13]). Although the core structure of the protein is not adversely affected by the truncation of the intersubunit lock-and-key motif, the mutation does impact significantly on protein function indicating that tertiary structural changes have occurred at/near the active and non-substrate ligand-binding sites of the mutant protein.

The fact that the F51S mutant protein bound very weakly to the *S*-hexylglutathione-affinity column was evidence for the presence of a structurally compromised active site. Furthermore, kinetics data confirmed that the conformations of both the G- and H-sites (i.e. the glutathione-binding and hydrophobic substrate-binding sites, respectively) were altered with the G-site being disrupted to the greatest extent. Phe-51 is located in a loop connecting α-helix 2 and β-strand 3 of domain I. Both secondary structural moieties as well as elements of the loop form part of the G-site (Fig. 1A); Arg-44 in α-helix 2 forms a salt bridge with the glycine moiety of glutathione and a pair of antiparallel β-strand hydrogen bonds form between the backbone of glutathione at its cysteinyl moiety and the protein backbone at Val-54 [20]. Val-54 precedes an invariant *cis*-Pro-55 motif at the N-terminus of β-strand 3. Helix 2 makes tertiary interactions with helix 9 located at the C-terminus of the A1 polypeptide [10,20]. Helix 9, a unique dynamic structural feature in class alpha GSTs, is a structural part of the H-site for electrophilic substrates [22]. The lock-and-key motif most likely restricts the conformational flexibility of helix 2 and, therefore, indirectly modulates the dynamics of helix 9.

The lock-and-key intersubunit motif in hGSTA1-1 also impacts on the binding of the non-substrate ligand ANS. This anionic dye binds an amphipathic region at the dimer interface [16] that is similar to that for aflatoxin B1 [17], β-estradiol disulfate [23] and AEDANS [11,17]. For wild-type protein, the binding of glutathione to the G-site enhances binding of ANS (Fig. 2; [24]). The binding sites for these ligands, therefore, do not overlap. This enhanced binding effect is attributed to a glutathione-induced immobilization of helix 9 onto domain I allowing the C-terminus of the GSTA1 polypeptide to contribute toward the ligandin site for ANS [24]. In the absence of glutathione, F51S mutant hGSTA1-1 binds more ANS than wild-type protein. Disruption of the lock-and-key interaction exposes hydrophobic surface that, according to the emission maxima for the bound dye, appears to be more hydrophobic than for the ANS site in the wild-type protein.

The F51S mutant protein displays diminished conformational stability. The protein concentration dependence of the unfolding data suggests the presence of (a) highly populated dimeric state(s) in equilibrium with unfolded monomer within the urea unfolding transition. The lock-and-key motif, therefore, although not essential for dimerization to occur, stabilizes the quaternary structure at the dimer interface. Possible reasons for a reduced *m*-value for hGSTA1-1 have been given [13]. In the light of the enhanced exposure of hydrophobic surface in the mutant protein, it is possible that the initial state of the mutant protein prior to unfolding has a larger solvent accessible surface area than the wild-type protein, thus resulting in a diminished dependence of the Gibbs free energy of unfolding on urea concentration. At this stage, the exact nature of the structural changes induced by the F51S mutation is not clear.

Acknowledgements: Financial support was received from the University of the Witwatersrand, the Andrew Mellon Foundation and the South African National Research Foundation.

References

[1] Mannervik, B. and Danielson, U.H. (1988) CRC. Crit. Rev. Biochem. Mol. Biol. 23, 283–337.
[2] Dirr, H., Reinemer, P. and Huber, R. (1994) Eur. J. Biochem. 220, 645–661.
[3] Ji, X., von Rosenvinge, E.C., Johnson, W.W., Tomarev, S.I., Piatagorsky, F., Armstrong, R.N. and Gilliland, G.L. (1995) Biochemistry 34, 5317–5328.
[4] Meyer, D.J., Coles, B., Pemble, S.E., Gillmore, K.S., Fraser, G.M. and Ketterer, B. (1991) Biochem. J. 274, 409–441.
[5] Pemble, S.E., Wardle, A.F. and Taylor, J.B. (1996) Biochem. J. 319, 754–759.
[6] Board, P.G., Baker, R.T., Chelevanayagam, G. and Jermiin, L.S. (1997) Biochem. J. 328, 929–935.
[7] Erhardt, J. and Dirr, H. (1995) Eur. J. Biochem. 230, 614–620.
[8] Stevens, J.M., Hornby, J.A.T., Armstrong, R.N. and Dirr, H.W. (1998) Biochemistry 37, 15534–15541.
[9] Stenberg, G., Bjornstedt, R. and Mannervik, B. (1992) Proteins Expr. Purif. 3, 80–84.
[10] Cameron, A.D., Sinning, I., L'Hermite, G., Olin, B., Board, P.G., Mannervik, B. and Jones, T.A. (1995) Structure 3, 717–727.
[11] Wallace, L.A., Sluis-Cremer, N. and Dirr, H.W. (1998) Biochemistry 37, 5320.
[12] Dirr, H.W. and Reinemer, P. (1991) Biochem. Biophys. Res. Commun. 180, 294–300.
[13] Wallace, L.A., Blatch, G.L. and Dirr, H.W. (1998) Biochem. J. 336, 413–418.
[14] Bico, P., Erhardt, J., Kaplan, W. and Dirr, H. (1995) Biochim. Biophys. Acta 1247, 225–230.
[15] Pace, C.N. (1986) Methods Enzymol. 131, 266–280.
[16] Sluis-Cremer, N., Naidoo, N.N., Kaplan, W.H., Manoharan, T.H., Fahl, W.E. and Dirr, H.W. (1996) Eur. J. Biochem. 241, 484–488.
[17] Sluis-Cremer, N., Wallace, L.A., Burke, J., Stevens, J. and Dirr, H. (1998) Eur. J. Biochem. 257, 434–442.
[18] Semisotnov, G.V., Rodionova, N.A., Kutyshenko, V.P., Ebert, B., Blank, J. and Ptitsyn, O.B. (1987) FEBS Lett. 224, 9–13.
[19] Kaplan, W., Husler, P., Klump, H., Erhardt, J., Sluis-Cremer, N. and Dirr, H.W. (1997) Protein Sci. 6, 399–406.
[20] Sinning, I., Kleywegt, G.J., Cowan, S.W., Reinemer, P., Dirr, H.W., Huber, R., Gilliland, G.L., Armstrong, R.N., Ji, X., Board, P.G., Olin, B., Mannervik, B. and Jones, T.A. (1993) J. Mol. Biol. 232, 192–212.
[21] Armstrong, R.N. (1997) Chem. Res. Toxicol. 10, 2–18.
[22] Board, P.G. and Mannervik, B. (1991) Biochem. J. 275, 171–174.
[23] Barycki, J.J. and Colman, R.F. (1997) Arch. Biochem. Biophys. 345, 16–31.
[24] Dirr, H.W. and Wallace, L.A. (1999) Biochemistry 38, 15631–15640.
[25] Wallace, L.A. and Dirr, H.W. Biochemistry, article BI991239Z, in press.